

**Supporting Information for**

**Efficient High Active Mass Paper-Based Energy Storage Devices containing  
Free-standing Additive-less Polypyrrole-Nanocellulose Electrodes**

Zhaohui Wang,\* Petter Tammela, Peng Zhang, Maria Strømme\* and Leif Nyholm\*

Dr. Z.H. Wang, Prof. L. Nyholm

Department of Chemistry-The Ångström Laboratory, Uppsala University, Box 538,  
SE-751 21 Uppsala, Sweden

E-mail: [zhaohui.wang@kemi.uu.se](mailto:zhaohui.wang@kemi.uu.se); [leif.nyholm@kemi.uu.se](mailto:leif.nyholm@kemi.uu.se)

P. Tammela, P. Zhang, Prof. M. Strømme

Nanotechnology and Functional Materials, Department of Engineering Sciences, The  
Ångström Laboratory, Uppsala University, Box 534, SE-751 21 Uppsala, Sweden

E-mail: [maria.stromme@angstrom.uu.se](mailto:maria.stromme@angstrom.uu.se)

## **Experimental Section**

### ***Materials Synthesis***

Cladophora green algae were collected from the Baltic Sea and the nanocellulose was extracted using grinding and acid hydrolysis as previously described.<sup>[1, 2]</sup> Iron (III) nitrate nonahydrate ( $\text{FeNO}_3 \cdot 9\text{H}_2\text{O}$ ), concentrated nitric acid ( $\text{HNO}_3$ ), hydrochloric acid ( $\text{HCl}$ ), ammonium persulfate (APS), cetrimonium bromide (CTAB,  $(\text{C}_{16}\text{H}_{33})\text{N}(\text{CH}_3)_3\text{Br}$ ), sodium nitrate ( $\text{NaNO}_3$ ), lithium nitrate ( $\text{LiNO}_3$ ), pyrrole (Py) and Tween-80 were purchased from Sigma-Aldrich and used as received. Deionized water was used throughout the synthesis.  $\text{LiFePO}_4$  powder was purchased from Phostech Lithium, Inc., Montreal, Canada. Filter papers (Munktell, Sweden, General purpose filter papers) were used as obtained from Sigma-Aldrich.

***Preparation of interconnected PPy nanofiber:*** interconnected PPy nanofibers were synthesized using a previously reported <sup>[3, 4]</sup> modified oxidative template assembly route. Typically, 7.3 g CTAB was first dissolved in 1 M HCl solution (120 mL) on an ice bath and 13.7 g APS was then added to immediately yield a white reactive template. After stirring for 30 minutes and cooling down to 0-5 °C, pyrrole (8.3 mL) was added to the as-formed reactive template solution. The reaction between the pyrrole and the APS was carried out at 0-5 °C for 24 hours. A black precipitate composed of the polypyrrole nanofiber was obtained. This precipitate was washed with 1 M HCl and deionized water until the filtrate was colorless and neutral. The interconnected PPy nanofiber was finally dried overnight at 80 °C in an oven.

***Preparation of PPy@nanocellulose composite:*** Cladophora cellulose (40 mg)

was dispersed in water (8 mL) by sonication for a total pulse time of 10 min with water cooling. The sonication was carried out using high-energy ultrasonic equipment (Sonics and Materials Inc., USA, Vibra-Cell 750) at an amplitude of 30% with a pulse length of 30 s and pulse-off duration of 30 s. Pyrrole (0.135 mL), Tween-80 (one drop) and 0.5 M nitric acid (6 mL) were mixed with the cellulose dispersion employing magnetic stirring for 5 min. Polypyrrole was then formed on the Cladophora cellulose fibers by chemical polymerization employing iron (III) nitrate (1.15 g) dissolved in 0.5 M nitric acid (8 mL) as the oxidant. The polymerization was allowed to proceed for 30 min under stirring after which the composite was collected in an Büchner funnel connected to a suction flask and washed with 0.5 M nitric acid (1 L) followed by 0.1 M NaNO<sub>3</sub> (0.1 L). The washed composite was kept well-dispersed in a stirred solution prior to further use. To estimate the weight of the as-prepared PPy@nanocellulose composites, another batch of PPy@nanocellulose materials was analogously prepared, collected on a filter paper, pressed, and left to dry in open air. The weight of this material was about 135 mg. The cellulose and PPy mass percentages in the composites were estimated at 30 % and 70 %, respectively, by weighting the PPy@nanocellulose powder before and after the polymerization, which is in good agreement with our previous studies.<sup>[1, 5]</sup>

***Preparation of PPy nanofiber-PPy@nanocellulose paper electrodes:*** 250 mg PPy nanofiber was dispersed in 50 mL DI water by sonication for 1 minute followed by stirring for 30 minutes. The as-prepared PPy@nanocellulose suspension was then added to the previous solution, sonicated for 1 minute and mixed using a mechanical

homogenizer (IKA T25 Ultra-Turrax, Germany) at 6800 rpm for 10 minutes. The mixture was then drained on a filter paper to form a filter cake and subsequently dried to form a paper sheet. In this study, the PPy nanofiber mass ratio was calculated as the  $(\text{mass of PPy nanofiber})/(\text{mass of PPy nanofiber} + \text{mass of PPy@nanocellulose})$ , yielding a value of 65 wt.%, whereas the cellulose mass ratio was calculated from the  $(\text{mass of cellulose})/(\text{mass of PPy nanofiber} + \text{mass of PPy@nanocellulose})$ , resulting in a value of ~10 wt. %. This gives a cellulose:PPy mass ratio in the composite of 1:9, i.e. an electroactive mass fraction of 90 %.

***Preparation and use of LiFePO<sub>4</sub>-PPy@nanocellulose paper electrodes:*** The preparation of LiFePO<sub>4</sub>-PPy@nanocellulose paper electrodes is analogous to the synthesis of PPy nanofiber-PPy@nanocellulose except for the fact that 100 mg LiFePO<sub>4</sub> (LFP) powder also is included in the synthesis. The weight fraction for the LiFePO<sub>4</sub> was estimated to be 42%, while that the active material (i.e. LiFePO<sub>4</sub>+PPy) was around 82%.

### ***Material and Electrochemical Characterizations***

Scanning Electron Microscopy (SEM) micrographs for all samples were obtained employing a Leo Gemini 1550 FEG SEM instrument (UK) whereas the specific surface areas of the composites were obtained with a ASAP 2020 instrument (Micromeritics, USA) using a multipoint Brunauer-Emmett-Teller (BET) approach involving N<sub>2</sub> gas adsorption isotherms analysis. Fourier transform infrared (FTIR) spectra were recorded using a Spectrum One FTIR spectrometer equipped with a Diamond/ZnSe crystal (PerkinElmer, U.S.).

The electrochemical performance of paper electrode was studied with cyclic voltammetry and galvanostatic charge-discharge measurements at room temperature employing an Autolab/GPES instrument (ECO Chemie, The Netherlands).

**Cyclic voltammetry:** The cyclic voltammetry (CV) measurements were performed with the synthesized paper electrode as the working electrode in a three-electrode electrochemical cell where a platinum wire served as the counter electrode and an Ag/AgCl electrode was used as the reference electrode. The paper samples used as the working electrode were cut out pieces weighing about 4 mg, which were contacted by a platinum wire coiled around the sample. A solution of 2 M NaCl, purged with nitrogen for 15 min prior to the measurements, was used as the electrolyte. In the charge capacity calculations all values were normalized with respect to the total mass of the composite.

**Fabrication of the paper-based supercapacitor devices:** A piece of ordinary filter paper, used as a separator, was sandwiched between two rectangular pieces (0.9 cm long and 0.8 cm wide, weighing ~16 mg each) of the composite paper material. The composite electrodes of this symmetrical electrochemical cell were contacted using two glassy carbon plates covering the entire surface of the paper electrode which in turn were connected to the platinum foil current collector strips. To assure good electrical contact, the entire device was then tightly clamped between two plastic plates leaving a small (1-2 mm) gap between the plastic plates. The entire cell was then immersed into 40 mL of a 2 M NaCl solution. Different current densities between 1.35 mA cm<sup>-2</sup> and 270 mA cm<sup>-2</sup> (corresponding to 0.085 to 16.8 A g<sup>-1</sup> based

on the weight of one electrode) were then applied while a current density of 25 mA cm<sup>-2</sup> (i.e. 1.56 A g<sup>-1</sup>) was used for the cycling stability tests, as the cell was charged to a voltage of 0.8 V.

The cell capacitances of the symmetric supercapacitor devices were derived from the galvanostatic discharge curves according to  $C = I\Delta t/\Delta V$ , where  $C$  denotes the device capacitance,  $I$  the discharge current and  $\Delta V$  represents the potential change within the discharge time  $\Delta t$ . The mass-specific cell capacitances were calculated as  $C_m=C/M$ , where  $M$  refers to the total mass of the two paper composite electrodes. The area-normalized cell capacitances were estimated as  $C_s=C/S$ , where  $S$  denotes the geometric area of the electrodes. The device energy density was calculated using  $E = 1/2 C_m (\Delta V)^2$  while the power density was derived from  $P = E/\Delta t$ .

### **Theoretical specific capacitance, energy density and power density for PPy**

The theoretical capacity for polypyrrole is 360 C g<sup>-1</sup> (PPy) for 25% doping<sup>[6]</sup> and in the calculations below this doping degree was assumed to be obtained at +0.6 V vs. Ag/AgCl. This yields a theoretical capacitance of 600 F g<sup>-1</sup>.<sup>[6]</sup> While the use of higher potentials clearly should give larger capacities the capacitance should remain the same, at least at potentials where the influence of the overoxidation reaction is small (i.e. at potentials up to about +0.6 V vs. Ag/AgCl).

Given that the stored energy ( $W$ ) is given by  $W=0.5 \cdot U^2 \cdot C = 0.5 \cdot Q \cdot U$  (where  $U$  denotes the voltage,  $C$  the capacitance and  $Q$  the charge), the theoretical energy density for a PPy electrode at +0.6 V vs. Ag/AgCl is thus equal to 30 Wh kg<sup>-1</sup> (PPy).

$$360 \cdot 0.6 \cdot 0.5 = 108 \text{ Ws g}^{-1} = 108/3600 \text{ Wh g}^{-1} = 0.03 \text{ Wh g}^{-1} = 30 \text{ Wh kg}^{-1}$$

For a symmetric two-electrode device in which the two electrodes both are charged to 0.4 V (yielding a cell voltage of 0.8 V), a theoretical energy density of 3.3 Wh kg<sup>-1</sup> (PPy) is, on the other hand, obtained after normalisation with respect to the weight of both electrodes (see below). Note that only half of the energy of the electrodes can be utilised in a symmetric device and that the attainable charge at 0.4 V has been assumed to be proportionally lower than at 0.6 V vs. Ag/AgCl.

$$(360 \cdot 0.4/0.6) \cdot 0.4 \cdot 0.5 \cdot 0.5 \cdot 0.5 = 12 \text{ Ws g}^{-1} = 12/3600 \text{ Wh g}^{-1} = 3.3 \text{ Wh kg}^{-1}.$$

If the potential distribution in the device is different, i.e. not symmetrical, the value will be reduced further as the smaller value would determine the attainable energy density. Our previous findings, however, indicate that it is reasonable to assume a symmetrical distribution for the present type of devices. Assuming an energy density for a device of 3.3 Wh/kg PPy and a discharge time of 1.2 s yields a power density of 10 kW kg<sup>-1</sup> as demonstrated below:

$$3.3 \text{ Wh kg}^{-1} = 0.0033 \text{ Wh g}^{-1} = 12 \text{ Ws g}^{-1} = 12 \text{ kWs kg}^{-1}$$

Discharge during 1.2 s thus yields a power density of 10 kW kg<sup>-1</sup>.

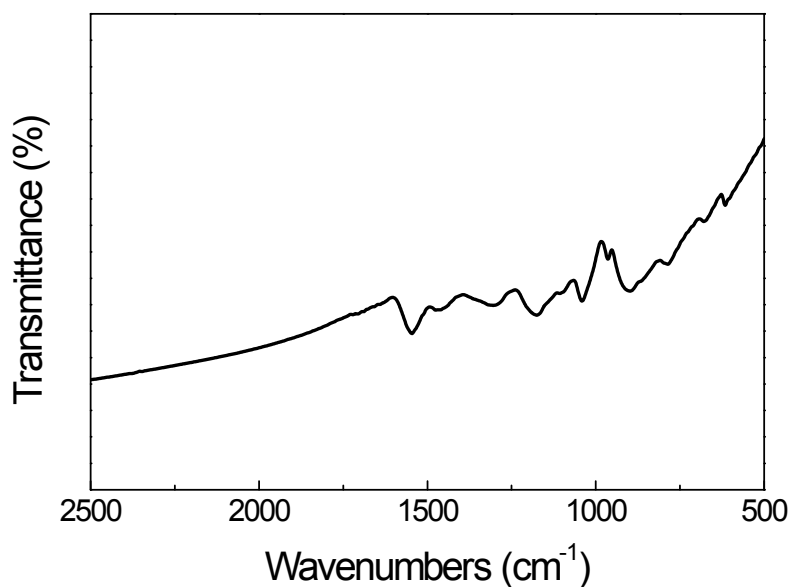


Fig. S1. FTIR spectrum for the PPy nanofibers.

The characteristic peaks at 1546 and 1461  $\text{cm}^{-1}$  are attributed to the C=C and C-N stretching deformation mode of the pyrrole rings while the characteristic band at 900  $\text{cm}^{-1}$  is related to the C-H out-plane vibration. The bands at 1300 and 1037  $\text{cm}^{-1}$  could be interpreted as stemming from C-H in-plane vibration and in-plane N-H deformation, respectively whereas the 1174  $\text{cm}^{-1}$  band could be due to a C-N-C stretching vibration in the polaron structure.<sup>[3, 7]</sup> The obtained FTIR spectrum thus demonstrates that PPy was indeed present in the PPy nanofibre sample.

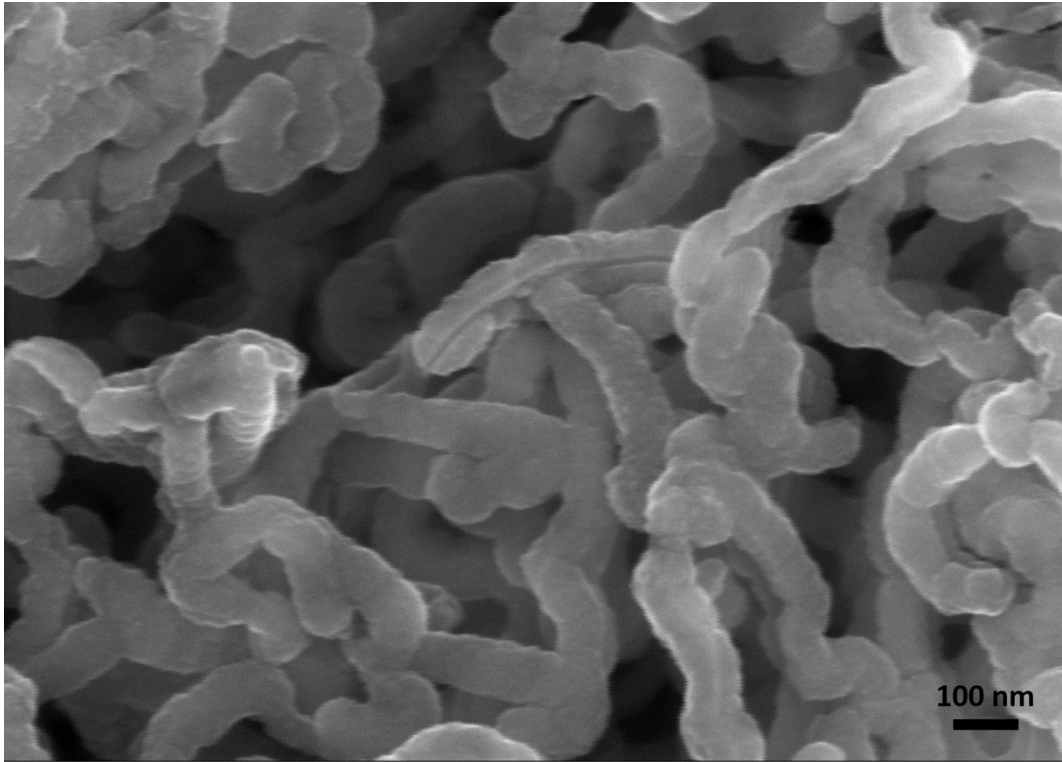


Fig. S2. High magnification SEM micrograph of the PPy nanofibers.

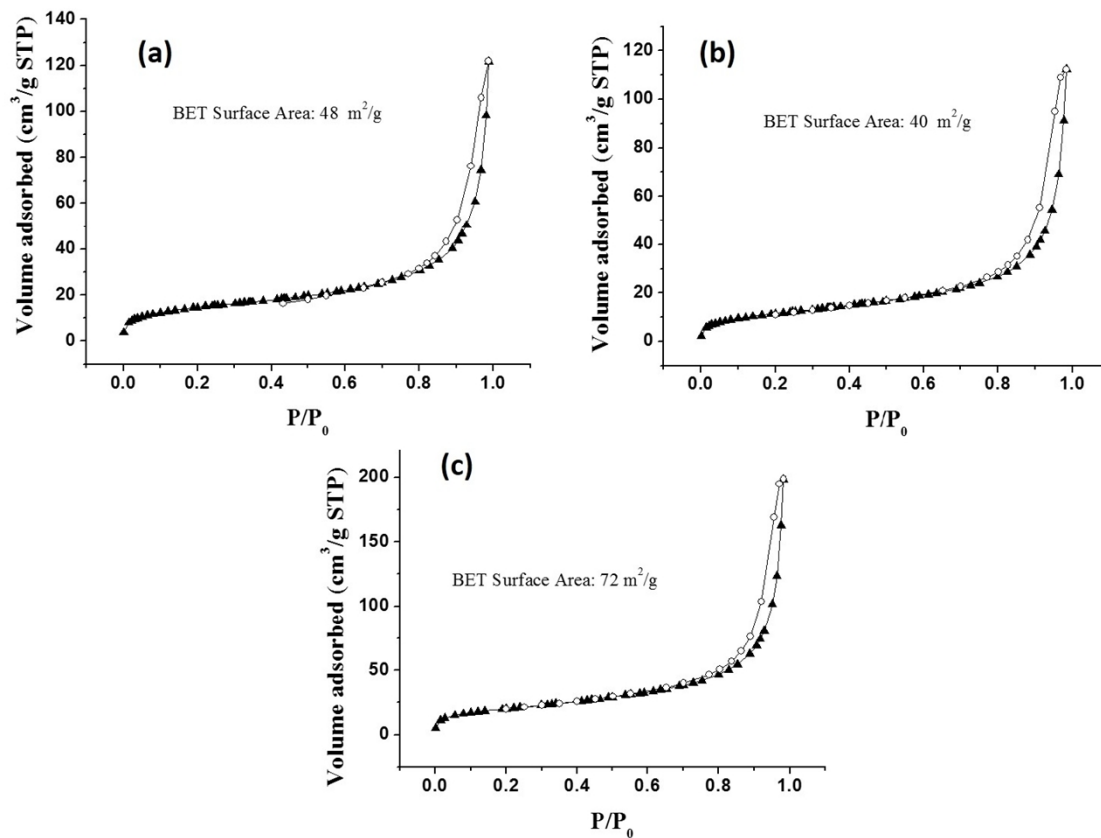


Fig. S3. Nitrogen adsorption/desorption isotherms for (a) PPy nanofibres, (b) PPy nanofibre-PPy@nanocellulose composite and (c) PPy@nanocellulose. The BET surface area of each sample type is displayed.

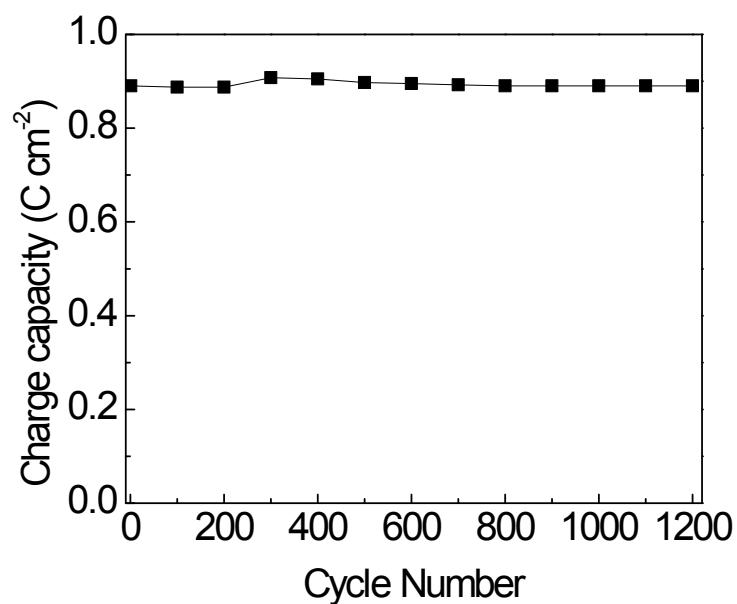


Fig. S4. Cell capacity vs. cycle number obtained from a 1200 cycle charge/discharge cycling test performed with a current density of 25 mA cm<sup>-2</sup>.

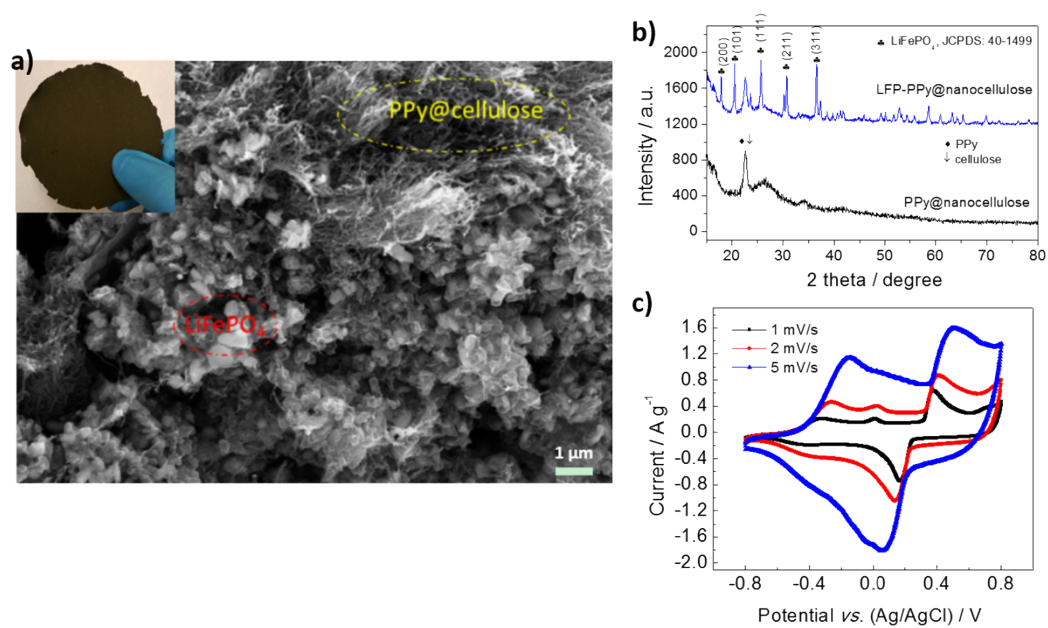


Fig. S5. (a) SEM image of the LiFePO<sub>4</sub>-PPy@nanocellulose composite, (b) XRD for LiFePO<sub>4</sub>-PPy@nanocellulose and PPy@nanocellulose, respectively and (c)

a cyclic voltammogram recorded for the LiFePO<sub>4</sub>-PPy@nanocellulose composites in 5 M aqueous LiNO<sub>3</sub>.

This synthesis strategy described in the present work can readily be extended to also include other electroactive materials, such as LiFePO<sub>4</sub>. As demonstrated by SEM and XRD (see Fig. S5a and Fig.S5b), the LiFePO<sub>4</sub> particles were supported by the PPy@cellulose 3D matrix, yielding an additive-free, self-standing electrode. The inset in panel a) shows a photograph of the paper-like composite obtained after mixing PPy@nanocellulose and LiFePO<sub>4</sub>. Fig. S5b shows the X-ray diffraction pattern of the PPy@nanocellulose and LiFePO<sub>4</sub> hybrid composites. The main peaks for PPy@nanocellulose seen in the PPy/nanocellulose spectra match previous reported cellulose/PPy data well.<sup>[8]</sup> The cyclic voltammograms for the LiFePO<sub>4</sub>-PPy@nanocellulose hybrid electrode (Fig. S5c), recorded in 5 M LiNO<sub>3</sub> aqueous electrolyte at scan rates from 1 mV s<sup>-1</sup> to 5 mV s<sup>-1</sup> between -0.8 V and 0.8 V (vs. Ag/AgCl) are likewise shown in Figure S5. In addition to the redox peaks for PPy, an additional pair of oxidation and reduction peaks at ~ +0.36 and +0.17 V (vs. SCE), respectively, was clearly observed for the lowest scan rate due to the extraction/insertion of lithium ions from/into LiFePO<sub>4</sub> in the aqueous electrolyte.<sup>[9]</sup> This indicates that this type of LiFePO<sub>4</sub> composites can be used in Li-ion batteries although the positive shift in the oxidation peaks for increasing scan rates indicates that these materials need some further optimization. This work will focus on the preparation of a uniform distribution of LiFePO<sub>4</sub> and PPy@nanocellulose and the elimination of O<sub>2</sub> from the aqueous electrolyte.

## References

- [1] G. Nystrom, A. Razaq, M. Stromme, L. Nyholm, A. Mihranyan, *Nano Lett* **2009**, 9, 3635.
- [2] A. Mihranyan, A. P. Llagostera, R. Karmhag, M. Strømme, R. Ek, *International Journal of Pharmaceutics* **2004**, 269, 433.
- [3] Z. Wang, X. Xiong, L. Qie, Y. Huang, *Electrochimica Acta* **2013**, 106, 320.
- [4] Z. Wang, L. Qie, L. Yuan, W. Zhang, X. Hu, Y. Huang, *Carbon* **2013**, 55, 328.
- [5] D. O. Carlsson, G. Nyström, Q. Zhou, L. A. Berglund, L. Nyholm, M. Strømme, *Journal of Materials Chemistry* **2012**, 22, 19014.
- [6] L. Nyholm, G. Nyström, A. Mihranyan, M. Strømme, *Advanced Materials* **2011**, 23, 3751.
- [7] H. Mi, Y. Xu, W. Shi, H. Yoo, S. Park, Y. Park, S. M. Oh, *Journal of Materials Chemistry* **2011**, 21, 19302.
- [8] D. Müller, C. R. Rambo, D.O.S.Recouvreux, L. M. Porto, G. M. O. Barra, *Synthetic Metals* **2011**, 161, 106.
- [9] M. Zhao, B. Zhang, G. Huang, H. Zhang, X. Song, *Journal of Power Sources* **2013**, 232, 181.